Electrochimica Acta 331 (2020) 135319

Contents lists available at ScienceDirect

Electrochimica Acta

journal homepage: www.elsevier.com/locate/electacta

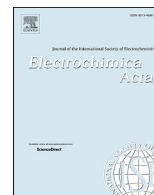

The effect of anions on the anodic formation of copper sulphide films on copper

T. Martino [a], J. Chen [a, *], J.J. Noël [a, b], D.W. Shoesmith [a, b]

[a] Department of Chemistry, The University of Western Ontario, London, Canada
[b] Surface Science Western, The University of Western Ontario, London, Canada

ARTICLE INFO

Article history:
Received 4 October 2019
Received in revised form
7 November 2019
Accepted 16 November 2019
Available online 20 November 2019

Keywords:
Copper
Corrosion
Cyclic voltammetry
Aqueous sulphide
Anions

ABSTRACT

The influence of anions (Cl^-, SO_4^{2-}, HCO_3^-) on the anodic formation of Cu_2S films on Cu was investigated using cyclic voltammetry at rotating disk electrodes. At low ionic strengths, film growth was partially or completely controlled by ionic migration within pores in the growing film depending on the sulphide concentration. At low sulphide concentrations and high ionic strengths, film growth was controlled by the rate of anodic formation of Cu^I (as adsorbed $Cu(SH)_{ads}$) at the base of pores in the Cu_2S film. The ability of anions to suppress this reaction was in the order $SO_4^{2-} > HCO_3^- > Cl^-$. At higher sulphide concentrations, the film porosity was significantly reduced and film growth controlled by the properties of the compact Cu_2S film with ionic migration rate-controlling even at high ionic strength.

© 2019 Published by Elsevier Ltd.

1. Introduction

Copper is the primary candidate material for the manufacture of nuclear waste containers in Sweden, Finland and Canada since it is expected to be stable in the anoxic aqueous environments anticipated in deep geological repositories (DGR) [1–3]. The containers are comprised of two main components: a cast iron or carbon steel inner vessel and an outer Cu shell, which in combination are designed to avoid both corrosion and mechanical failure. In the Swedish/Finnish design, the outer shell would be fabricated using Cu with a thickness of 50 mm [2–4]. A small addition of P (30–100 ppmw) improves the creep properties, thereby limiting the probability for mechanical failure of the container after emplacement [5].

Although Cu is chosen for its resistance to corrosion in anoxic environments [1–3], Swedish and Finnish repositories are known to contain SH^-, formed in the groundwater as a consequence of sulphate-reducing bacteria and mineral dissolution processes [1–4,6]. Based on analyses of samples from boreholes in the proposed Swedish Forsmark repository, a $[SH^-]$ up to 1.4×10^{-4} M was measured [7], which is potentially detrimental to the container since SH^- can act as an oxidant for Cu producing a chalcocite (Cu_2S) film. However, various additional anions with comparable or greater concentrations will be present in the groundwater and would be expected to influence the Cu_2S film growth process. The groundwater anions of dominant interest, and their expected concentrations (after 10,000 years) in the DGR, are chloride (3×10^{-4} M to 0.154 M), bicarbonate (3×10^{-4} M to 5×10^{-3} M), and sulphate (2×10^{-4} M to 7.2×10^{-3} M), respectively [2].

Chen et al. studied the effects of $[Cl^-]$ on Cu corrosion in quiescent anoxic SH^- solutions containing 10^{-3} M SH^- [8]. It was shown that the Cu_2S film properties were significantly altered when the $[Cl^-]$ was increased. At a relatively low $[Cl^-]$ (0.1 M), the film grew according to a logarithmic growth law and displayed protective properties. On increasing the $[Cl^-]$ to 0.5 M, the film developed a more porous structure, as indicated by electrochemical impedance spectroscopy (EIS) and confirmed by scanning electron microscopy (SEM) performed on focused ion beam (FIB) cut cross sections. Additionally, a linear film growth rate indicated the film was not protective, providing further evidence of porosity. At the highest concentration studied, 5.0 M, the Cu_2S film developed extensive porosity, and film growth appeared to be governed by a combination of SH^- diffusion in the bulk solution and the transport of soluble Cu^I species ($Cu(SH)_2^-$ or Cu_3S_3 clusters [9,10]) in the pores of the film. This, and additional studies [6,11], indicate that Cl^- influences the Cu_2S growth process by displacing adsorbed SH^-

* Corresponding author.
E-mail address: jchen496@uwo.ca (J. Chen).

https://doi.org/10.1016/j.electacta.2019.135319
0013-4686/© 2019 Published by Elsevier Ltd.

from the Cu surface thus inhibiting the first step in the SH^- induced corrosion reaction.

Chen et al. also studied the key parameters that govern the properties and structure of the Cu_2S films grown in anoxic aqueous environments [12]. Concentrations of Cl^- ranging from 0.1 M to 5.0 M were studied in solutions with various $[SH^-]$ from 10^{-5} M to 10^{-3} M. The structure and properties of the films were determined by three critical factors: $[SH^-]$ and $[Cl^-]$, their ratio, and the flux of SH^- to the corroding Cu surface. The film structure and the kinetics of its growth were governed by competition between the interfacial reaction rate and the rate of SH^- diffusion. When the interfacial reaction (i.e., the generation of oxidized Cu species) was rate determining, the Cu_2S film was compact and protective, and when SH^- diffusion dominated, the film was porous and non-protective. A ratio of $[Cl^-]/[SH^-] \geq 1000$ appeared to be required for a switch from a compact to a porous film to be observed. However, it remains unclear whether or not similar behaviour will be observed when other anions are present.

When studied electrochemically [13,14], the properties of the Cu_2S film formed were also found to be dependent on $[SH^-]$ and $[Cl^-]$ and the transport of SH^- to the Cu surface (controlled using a rotating disc electrode (RDE)). At low $[SH^-]$, a thin single porous layer was formed, with a dual layer film developing as $[SH^-]$ was increased. For a sufficiently high $[SH^-]$ ($\geq 5 \times 10^{-4}$ M), the film appeared to become at least partially passive. A series of published studies in solutions containing $[SH^-] = 2 \times 10^{-4}$ M, has claimed that the film grown electrochemically at this $[SH^-]$ is a passive copper sulphide film [15–19]. However, more recent studies have demonstrated that the resistance to film growth is conferred by a deposited outer layer and not a passive barrier layer [20]. Further electrochemical studies demonstrated that the Cu_2S film formed remained porous and non-passive with passivity only achievable when oxide formation became possible at much more positive potentials [11].

The adsorption of various anions on Cu has been studied extensively, typically on single crystal electrodes. Broekmann et al. [21] studied the specific anion adsorption of Cl^- and SO_4^{2-} on a Cu(111) surface. It was shown that Cl^- caused an increased surface mobility of Cu atoms leading to a smoothing over of the holes, pits and islands observed after electropolishing. This mobility enabled large-scale morphological changes on a short time scale and became more pronounced as the applied potential was made more positive. In contrast, it was found that SO_4^{2-} adsorption did not allow for surface rearrangement and an overall low mobility of Cu was observed. Furthermore, SO_4^{2-} was found to adsorb in a close packed form with co-adsorbed species identified as H_2O, which is not surprising given the very large hydration enthalpy for this anion [22]. Lennartz et al. [23] found that SO_4^{2-} preferentially adsorbed on Cu(111) with a bidentate geometry. Scanning tunneling microscopy (STM) revealed a two-fold bridging adsorption site for the centers of the SO_4^{2-} molecules with C_{2V} symmetry. A study by Li and Nichols [24] found that the adsorbed SO_4^{2-} layer could be stabilized by structured hydration through incorporation of water via hydrogen bonding between adjacent SO_4^{2-} and co-adsorbed H_2O molecules. A study by Niaura and Malinaukas [25], using surface enhanced Raman spectroscopy (SERS), concluded that, on a roughened Cu electrode, the adsorption of Cl^- was preferred over that of SO_4^{2-}. Whether or not these differences in anion adsorption processes can influence Cu corrosion in the presence of SH^- has not been established.

The purpose of this study is to analyze the effect of various groundwater anions on the growth mechanism of Cu_2S films in aqueous SH^- solutions. This is of importance to degradation mechanisms of the container in the DGR because it would determine whether or not each individual groundwater anion (Cl^-, SO_4^{2-}, HCO_3^-/CO_3^{2-}) should be studied or whether the groundwater can be considered as one overall ionic electrolyte.

2. Experimental

2.1. Electrochemical cell and instrumentation

All electrochemical data were collected using a conventional three-electrode electrochemical glass cell. A Pt sheet rolled into a cylinder was used as the counter electrode and connected to external circuitry by a Pt wire. A saturated calomel electrode (SCE, 0.242 V/SHE) was used as the reference electrode. The cell was housed inside a Faraday cage to reduce electrical noise from external sources. All experiments were conducted using a rotating disk electrode (RDE). The electrode rotation rate was controlled by a Pine Instrument Company Analytical Rotator Model AFA86 Serial 882, and electrochemical measurements were made using a 1287 Solartron potentiostat connected to a computer equipped with CorrWare software.

2.2. Copper composition and electrode preparation

Oxygen-free, P-doped Cu provided by the Swedish Nuclear Fuel and Waste Management Co. (SKB), Solna, Sweden, was machined into Cu disks. Titanium rods were threaded into the back of the discs and the Cu was set into a Teflon holder using an epoxy resin. Only a single flat Cu face with a surface area of 0.785 cm^2 was exposed to solution. Prior to an experiment, the Cu electrode was first ground with a sequence of SiC papers with grit sizes: 1000, 1200, and 4000. Then, to achieve a mirror finish, the electrode was polished with Al_2O_3 suspensions with decreasing suspension size (1 μm, 0.3 μm, and 0.05 μm). The electrode was then rinsed thoroughly with Type-1 water (resistivity: 18.2 MΩ cm) and dried in a stream of ultrapure Ar gas (99.999%).

2.3. Solution preparation

Electrolyte solutions were prepared with Type-1 water obtained from a Thermo Scientific Barnstead Nanopure 7143 ultrapure water system. All water was purged with ultrapure Ar gas for 1 h prior to the preparation of solutions to prevent immediate oxidation of sulphide. Solutions were made from reagent-grade sodium sulphide nonahydrate ($Na_2S \cdot 9H_2O$, 98.0% assay) from Sigma Aldrich, sodium chloride (NaCl, 99.0% assay) and sodium carbonate (Na_2CO_3, 99.5% assay) from Caledon Laboratory Chemicals, sodium sulphate (Na_2SO_4, 101.5% assay) from Fisher Chemical, and sodium bicarbonate ($NaHCO_3$, 99.7–100.3% assay) from EMD Chemicals. To ensure an anoxic environment, solutions were Ar-purged for a minimum of 45 min before an experiment, with purging continued throughout the experiment.

2.4. Cyclic voltammetry experiments

Cyclic voltammetric (CV) studies were performed at a RDE. Prior to applying a voltammetric scan, the electrode was cathodically cleaned at −1.5 V/SCE to reduce air-formed oxides, and then at −1.15 V/SCE for a further 60 s to remove H_2 bubbles formed at the lower potential. Voltammetric scans were performed from an initial potential in the range −1.5 V/SCE to −1.35 V/SCE to an anodic limit between −0.7 V/SCE and −0.5 V/SCE, at a scan rate of 2 mV/s. The choice of starting potential had no influence on the subsequent electrochemical behaviour.

2.5. Auger electron spectroscopy (AES): depth profiling

Auger analyses were performed with a PHI 660 scanning Auger microprobe (SAM). A 5 keV primary electron beam rastered over a 100 μm × 100 μm area was used during Auger analysis. Depth profiling was performed using a 3 keV Ar^{+} ion beam rastered over a 2 mm × 2 mm area and the signal strength for Cu, S, O, C and Cl were monitored as a function of sputter time. Sputter time was converted into sputter depth using a sputter rate of 30 nm/min for a reference SiO_2 standard.

3. Results and discussion

3.1. The effect of chloride

3.1.1. The influence of chloride and sulphide concentration

Fig. 1 shows CVs recorded to an anodic limit of −0.70 V/SCE at an electrode rotation rate (ω) of 25 Hz in dilute (5 × 10^{-5} M and 10^{-4} M) SH^- solutions containing various chloride concentrations. At the low [SH^-] and this value of ω, when depletion of SH^- at the electrode surface would be expected, the anodic current slightly increased as the [Cl^-] increased from 0.1 M to 0.5 M. This was observed for both regions 1, when the current was dependent on potential, and 2 (Fig. 1a), when the current became independent of potential (as shown more clearly in Fig. 2). At higher [Cl^-] (≥1.0 M) the current in both anodic regions (1, 2) decreased substantially, as previously observed [11]. For all [Cl^-], the anodic current on the reverse scan was very close to that on the forward scan. This demonstrated that, as observed previously [13,14,20], the Cu_2S film formed on the forward scan was porous and did not limit the anodic formation of additional Cu_2S on the reverse scan. Integration of the positive and negative currents showed that all the charge consumed by the anodic formation of the film (Q_A) was recovered upon film reduction (Q_C), as observed previously [13].

The reduction of the Cu_2S film yielded a symmetrical cathodic peak (region 3 in Fig. 1a), which occurred at approximately the same potential for all chloride concentrations. This peak shape indicated that film reduction was distributed throughout the volume of the film, as expected for the nucleation and growth of Cu centers distributed within a porous film. Fig. 2 compares the dependence of the anodic plateau current (region 2) and the cathodic peak current (region 3) as a function of [Cl^-], confirming the direct relationship between the two, and showing that two distinct regions of film growth behaviour (A and B) were observed.

Similar anodic behaviour was observed at the intermediate

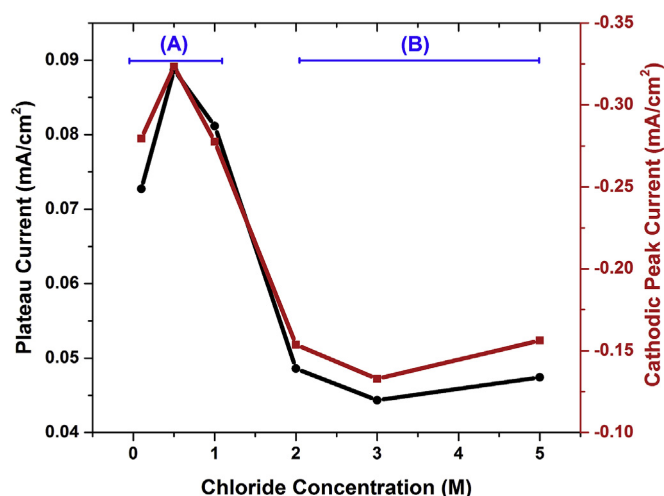

Fig. 2. Anodic plateau current (region 2 in Fig. 1a) and cathodic peak current (region 3 in Fig. 1a) obtained from CVs recorded in 5 × 10^{-5} M SH^- at ω = 25 Hz.

[SH^-] of 10^{-4} M, Fig. 1b; i.e., the current in both regions 1 and 2 first increased slightly with an increase in [Cl^-] before then decreasing. The values of Q_A and Q_C remained equal, as expected at the higher [SH^-], demonstrating that all the anodic charge was consumed in growth of the Cu_2S film. The anodic plateau and cathodic peak currents were considerably larger, but similarly related to those at the lower [SH^-]. The cathodic peak for film reduction was slightly asymmetrical at low [Cl^-] (0.1 M) and shifted to less negative potentials, becoming more symmetrical, as [Cl^-] increased. The anodic current in the plateau region (region 2, Fig. 1b) was not suppressed to the same extent as at the lower [SH^-], leading to much smaller differences in cathodic reduction peak currents and areas (region 3 in Fig. 1b) across the [Cl^-] range 0.1 M–5.0 M. This last observation suggested that the effect of Cl^- on the anodic film growth process was less dramatic at this slightly higher [SH^-] than at the lower [SH^-].

At the high [SH^-] of 2 × 10^{-3} M, distinctly different behaviour was observed, Fig. 3, although Q_A remained equal to Q_C. At low [Cl^-], the anodic current rose linearly with potential, before exhibiting a peak, as observed previously in experiments at high [SH^-] [13,20]. The film reduction peak subsequently recorded on the reverse scan (region 3 in Fig. 3) was also very asymmetrical with the large majority of film reduction occurring prior to the peak

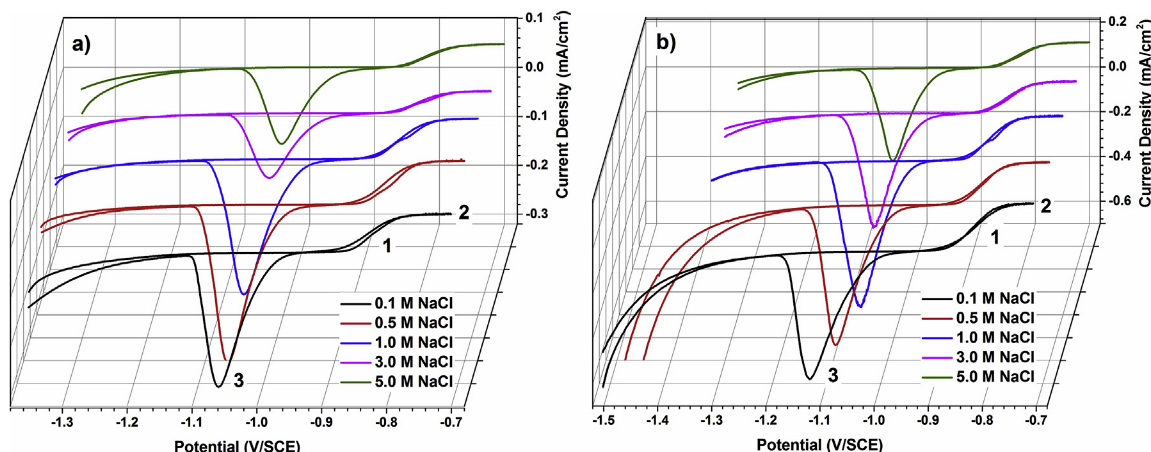

Fig. 1. CVs recorded at various [Cl^-] at ω = 25 Hz in solutions containing a) 5 × 10^{-5} M and b) 10^{-4} M SH^-.

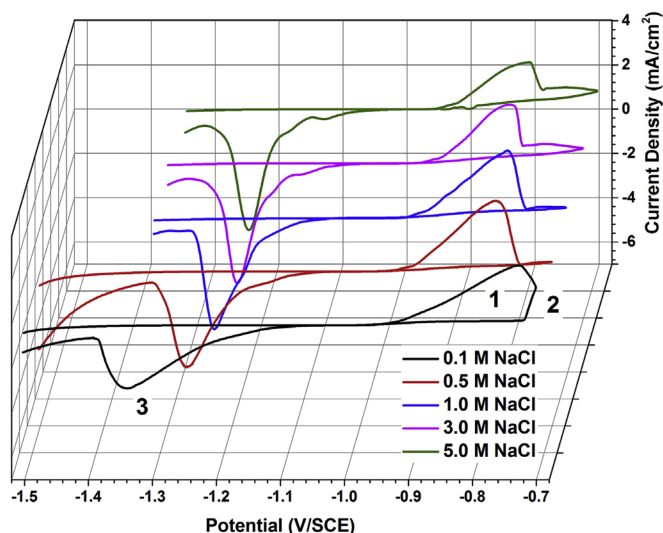

Fig. 3. CVs recorded at various [Cl^-] at ω = 25 Hz in a solution containing 2 × 10^{-3} M SH^-.

maximum, generally an indication of a compact film with reduction progressing from the film/Cu interface to the film/electrolyte interface.

The influence of [Cl^-] was more complex, Fig. 3, than observed at the two lower sulphide concentrations. At the lowest [Cl^-], both film growth and reduction appeared ohmically controlled, the current rising linearly with potential, suggesting the formation of a compact Cu_2S film. When [Cl^-] was increased, the linear increase in anodic current was retained but the current rose more rapidly with potential (region 1, Fig. 3) indicating a decreased resistance to film growth. As the peak was approached the current was suppressed as the [Cl^-] increased consistent with the observations at the two lower [SH^-]. After the subsequent decrease in current in region 2, the influence of [Cl^-] was inverted, the current increasing with [Cl^-] as shown in Fig. 4. Since EIS studies [20] showed the film remained porous in this potential region, the increased current suggested an influence of Cl^- on the porosity of the Cu_2S film/deposit as previously observed in corrosion experiments [9].

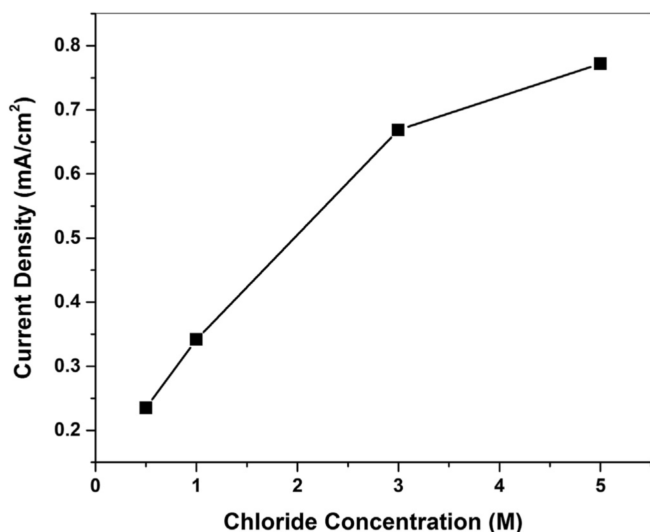

Fig. 4. Current densities for Cu_2S film formation at −0.75 V/SCE from CVs recorded in 2 × 10^{-3} M SH^- plotted as a function of [Cl^-].

Changes in the properties of the film with increasing chloride concentration were confirmed by three additional features. (i) A change in the shape of the film reduction peak, region 3 in Fig. 3, from asymmetrical to symmetrical. Both the peak symmetry and its shift in potential to less negative values indicated the film was both less compact and more easily reduced, most likely by a similar nucleation and growth process to that proposed for lower [SH^-]. (ii) The increase in the positive current recorded on the reverse scan (region 2) as the [Cl^-] was increased demonstrated the absence of passivation. (iii) A small reduction peak and shallow reduction shoulder developed at the higher [Cl^-]. These features have been observed and discussed previously [13], although their origin remains speculative.

It is clear from the features exhibited at the three [SH^-] that changes in [SH^-] and [Cl^-] exerted counterbalancing effects on film structure. As the [SH^-] increased at low [Cl^-], the film became more compact with an ohmically-controlled growth rate. This effect was from completely (at low [SH^-]) to partially (at high [SH^-]) offset by increases in [Cl^-] which led to more porous and readily reducible films.

Linear relationships between anodic film growth current and applied potential, similar to those observed in our study for [SH^-] = 2 × 10^{-3} M (Fig. 3), have been observed previously for the anodic formation of films on Ag involving large anions (SH^-, Br^-, and I^-) [26–28] and for the anodic formation of Ag_2O in alkaline solutions [29]. Such ohmic relationships were attributed to control of the film growth rate by ion migration within solution-filled pores in the growing film and not by the solid-state transport of Cu^+ species in a cation-conducting matrix. An influence of ionic migration would explain the increase in the anodic film growth current when the [Cl^-] was initially increased at the low [SH^-], Fig. 2. The increased ionic strength would lead to a decrease in the electric field within the solution filled pores, with the applied potential increasing across the Cu/solution interface at the base of the pores leading to an acceleration in the rate of anodic film formation.

An ionic strength effect cannot, however, account for the decrease in anodic film growth rate at lower [SH^-] and higher [Cl^-], Fig. 2, which suggested an interference of Cl^- with Cu_2S film growth, as its concentration was increased. That this interference was not due to the incorporation of Cl^- into the growing film, even in the most concentrated Cl^- solution (5.0 M), was clearly demonstrated by AES analyses, an example of which is shown in Fig. 5, which showed no Cl^- signal throughout the film.

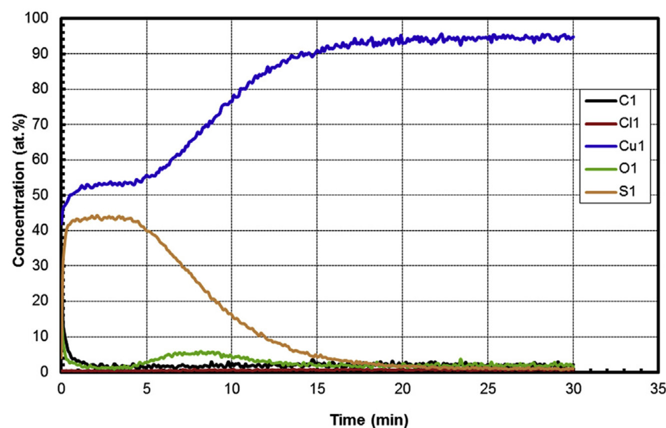

Fig. 5. Auger Depth Profile recorded on a Cu_2S film grown during a CV recorded in a 5.0 M Cl^- + 2.0 × 10^{-3} M SH^- solution at ω = 25 Hz up to an anodic potential limit of −0.7 V/SCE.

3.1.2. The influence of the sulphide to chloride concentration ratio

The nature of this interference by Cl^- could be seen in the changes in behaviour as the $[SH^-]/[Cl^-]$ ratio was changed. Since the equality between Q_A and Q_C indicated all the charge was consumed in film growth, either can be used as a measure of the extent of film growth. Consequently, the relative influence of Cl^- on the extent of film growth at various $[SH^-]$ could be appreciated by comparing Q_C for the film grown in 0.1 M Cl^- ($(Q_C)_{0.1}$), when the influence of Cl^- would have been the least, to Q_C for the film grown at other $[Cl^-]$ ($(Q_C)_{[Cl]}$). The ratio of these two charges ($R_Q = (Q_C)_{0.1}/(Q_C)_{[Cl]}$) then provided a relative measure of the influence of Cl^- on the film growth process at the different values of $[SH^-]$.

Fig. 6 shows this ratio, R_Q, calculated as a function of $[Cl^-]$ for the different sulphide concentrations. Two distinct regions of behaviour (A and B) were observed. In region A, when ionic migration within the porous Cu_2S film was partially rate controlling (Fig. 2, region A), a change in $[SH^-]$ had only a minor to negligible influence on film growth. For all three $[SH^-]$ an increase in R_Q was observed in the $[Cl^-]$ range 0.1–1.0 M, an effect that can be attributed to a contribution of ionic migration of SH^- to the current. At higher $[Cl^-]$ (i.e., as the $[Cl^-]/[SH^-]$ ratio increased) the suppression of Cu_2S formation, indicated by the decrease in R_Q (the vertical blue arrow in region B, Fig. 6), became considerably more marked. These observations were consistent with the behaviour observed under corrosion conditions for which it was shown that the film structure and kinetics of its growth changed with this concentration ratio [9]. Since, as noted above, the porosity increased as $[SH^-]$ was decreased, the greater suppression of the film growth by increases in $[Cl^-]$ at the lower $[SH^-]$ can be attributed to the more ready access of Cl^- to the Cu surface at the base of pores in the film. This increased the surface concentration of Cl^- and, hence, its ability to displace SH^- from adsorption sites on the Cu surface.

For the high ω (25 Hz) employed in these experiments, the lowest $[SH^-]$ at the Cu surface would have been achieved at the lowest bulk $[SH^-]$. According to the literature [30], Cl^- should not be as readily adsorbed on Cu as SH^-. However, at the extreme $[Cl^-]/[SH^-]$ ratios that would exist at the base of the pores in a Cu_2S film being anodically grown in a solution with a low $[SH^-]$, competition between Cl^- and SH^- for surface adsorption sites seemed likely.

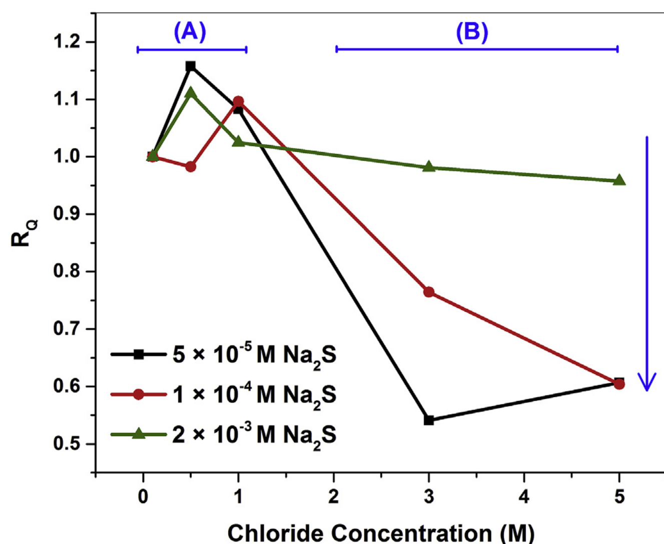

Fig. 6. Ratio (R_Q) (defined in the text) as a function of $[Cl^-]$ for three values of $[SH^-]$ recorded at ω = 25 Hz. The arrow indicates a suppression of anodic film growth as $[SH^-]$ increased. Regions A and B are the same as those defined in Fig. 2.

Also, a synergistic response was possible, since both Cl^- and SH^- complex Cu^I. Thus, the formation of Cu(I) by chemisorption of SH^- could have led to the co-adsorption of Cl^-, a process which could limit the release of Cu(I) (as $Cu(SH)_2^-$ or Cu_3S_3) to the solution.

The greater influence of ionic migration on the film growth rate at high $[SH^-]$, Fig. 3, can be attributed to a change in film porosity. At this high $[SH^-]$, the enhanced flux of SH^- into the porous film network led to a tighter porosity [27,28], an increased electric field within the film, a lower potential drop across the Cu/electrolyte interface at the base of pores, and, hence, a suppression of the anodic film growth. The suppression of anodic film growth by an increase in $[SH^-]$ but acceleration by an increase in $[Cl^-]$ at high potentials, Figs. 3 and 4, confirmed the contrasting influences of these anions on the film porosity with the properties of the films dominating the overall anodic behaviour rather than the interfacial reaction kinetics as observed when the film was more porous at lower $[SH^-]$.

3.1.3. Sulphide transport and chloride adsorption

For the two lower $[SH^-]$ for which the films were more porous and an influence of Cl^- on the interfacial rate was observed, the relative influences of SH^- transport and Cl^- surface adsorption can be appreciated from values of the ratio, R_D, of the current density (i_A) measured at −0.73 V/SCE (region 2, Fig. 3) to the theoretical diffusion limited current density (i_L) (calculated using the Levich equation) for the three $[SH^-]$ as a function of $[Cl^-]$ and at various values of ω, Fig. 7. In these plots a value of $R_D = 1$ indicated complete transport control, and $R_D = 0$ total rate control by the interfacial anodic reaction. At the lower $[Cl^-]$, for the lowest $[SH^-]$, Fig. 7a, R_D became slightly > 1 irrespective of the electrode rotation rate confirming a contribution to the current density of the ionic migration of SH^- within the pores in the film when the solution ionic strength was low. When $[Cl^-]$ was increased to > 1.0 M, R_D decreased as this contribution from ionic migration was eliminated at the higher ionic strength and diffusive transport became less important due to the influence of Cl^- adsorption suppressing the interfacial rate. At the intermediate $[SH^-]$, Fig. 7b, the contribution of ionic migration at the lowest $[Cl^-]$ was decreased, the measured current approaching the transport limited value except at the lowest ω when the diffusive contribution to SH^- transport would be at a minimum. These results indicate that the claim of diffusive control of the anodic formation of Cu_2S on Cu has limited application [31].

For both low and intermediate $[SH^-]$, R_D decreased to values well below 1 as $[Cl^-]$ was increased with a minor (low $[SH^-]$) or negligible (intermediate $[SH^-]$) dependence on ω. The lack of a dependence on ω indicated that the interfacial reaction current was directly dependent on the diffusion of SH^- to the Cu surface within the pores, with the dependence on $[Cl^-]$ a measure of the displacement of SH^- from surface adsorption sites by Cl^-.

3.2. The effect of sulphate and bicarbonate

Voltammograms recorded in a 10^{-4} M SH^- solution containing various $[SO_4^{2-}]$ are shown in Fig. 8a, and in a 2×10^{-3} M SH^- solution in Fig. 8b. The general shape of the curves was the same as observed in Cl^- solutions (Fig. 1). The anodic process was again reversible demonstrating that the Cu_2S film formed was porous with the anodic charge, Q_A, for Cu_2S formation equal to that for film reduction, Q_C, confirming that Cu_2S formation, continued on the reverse scan. The symmetrical shape of the cathodic reduction peak at the lower $[SH^-]$ (Fig. 8a) indicated, as observed at this $[SH^-]$ in Cl^- solutions, that the film reduction was distributed throughout the volume of the film as expected for the random nucleation and growth of Cu centers within a porous film.

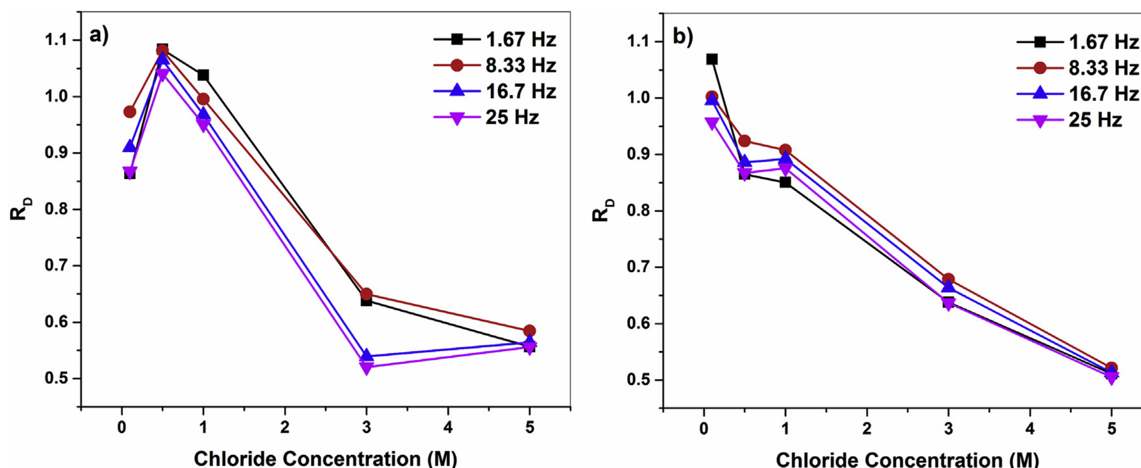

Fig. 7. Ratio (R_D) (defined in the text) as a function of [Cl^-] for various values of ω recorded in solutions of a) 5 × 10^{-5} M and b) 10^{-4} M SH^-.

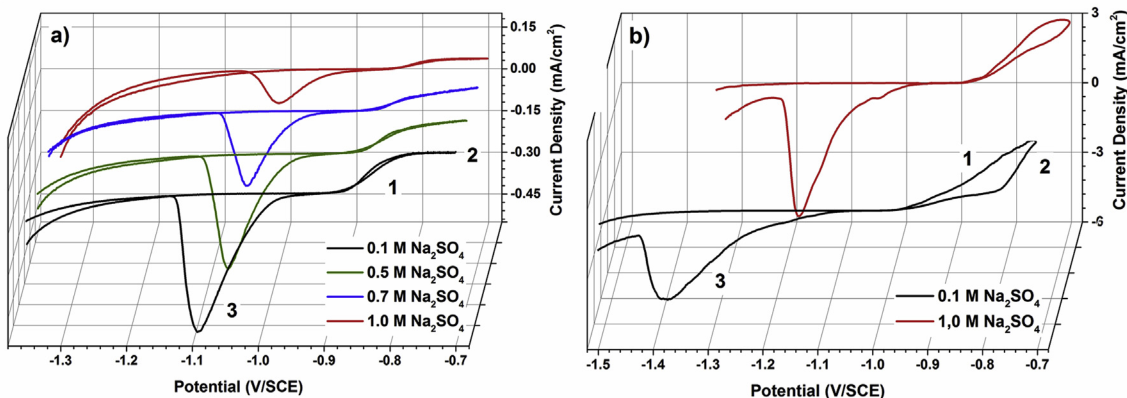

Fig. 8. CVs recorded in solutions containing various [SO_4^{2-}] at ω = 25 Hz with [SH^-] of a) 10^{-4} M and b) 2.0 × 10^{-3} M.

Despite this general similarity, a comparison of Figs. 1 and 8 shows a number of differences in behaviour in SO_4^{2-} compared to Cl^- solutions: (i) the potential at which anodic film formation commenced was more positive for SO_4^{2-} than Cl^- solutions (Figs. 1b and 8a). (ii) The current in region 2 was lower in SO_4^{2-} solutions than in Cl^- solutions, and the suppression of the current by increases in [SO_4^{2-}] was more marked than those imposed by increases in [Cl^-]; (iii) When [SH^-] was increased to 2 × 10^{-3} M, SO_4^{2-} exerted a similar influence to Cl^- on the evolution of the film reduction peak from asymmetrical to symmetrical accompanied by a shift to less negative potentials, Fig. 8b. As described above for Cl^- solutions, this last observation indicated a change in rate controlling process for film growth from ionic migration in pores at low [SO_4^{2-}] to the kinetics of the interfacial reaction at high [SO_4^{2-}].

Fig. 9 shows the ratio, R_D, as a function of [SO_4^{2-}] for the two [SH^-] and various values of ω. Comparison of Figs. 9a and 7b shows the values of R_D were considerably lower in the SO_4^{2-} than the Cl^- solution consistent with a greater influence of SO_4^{2-} on the interfacial anodic reaction rate. At the higher [SH^-] of 2 × 10^{-3} M a similar plot of R_D vs [SO_4^{2-}], Fig. 9b, confirmed the contribution of the ionic migration of SH^- ($R_D > 1.0$) at low ionic strengths (in 0.1 M SO_4^{2-}) and the suppression of anodic oxidation at high ionic strengths.

Inspection of Fig. 8b shows the fall in anodic current in region 2 observed in Cl^- solutions at high [SH^-] (Fig. 3c) did not occur in SO_4^{2-} solutions, suggesting the tightening of the porous structure observed at higher [SH^-]/[Cl^-] ratios was avoided in SO_4^{2-} solutions up to an anodic limit of −0.7 V/SCE. To confirm whether or not this was the case, CVs were performed to more positive potential limits in a concentrated SH^- solution (2 × 10^{-3} M) containing both Cl^- and SO_4^{2-}, Fig. 10. The anodic current was sustained up to −0.5 V/SCE, and was only marginally lower on the return scan, confirming that SO_4^{2-} interfered with the Cu_2S film growth process and prevented the formation of any surface protective layer. This indicated that the tightening of the film porosity which accounted for the suppression of the current in region 2 (Fig. 3) in Cl^- solutions at high [SH^-] did not occur when SO_4^{2-} was also present. This could be explained by the much lower anodic production rate of the transportable copper species ($Cu(SH)_2^-$ and Cu_3S_3), due to SO_4^{2-} adsorption on the Cu surface, which would limit the decreased porosity due to deposition on the walls of the pores in the growing film. A similar study was performed in solutions containing various [HCO_3^-]. Although not shown, suppression of anodic oxidation and the restructuring of the Cu_2S films similar to that exhibited in Cl^- and SO_4^{2-} were observed over the range 0.1 M ≤ [HCO_3^-] ≤ 1.0 M.

The influence of the various anions can most readily be compared by plotting the currents measured in region 2 as a function of anion concentration, Fig. 11. Over the concentration range, 0.1 M–1.0 M, the difference in behaviour of the two oxyanions compared to that of the Cl^- is clear for [SH^-] = 10^{-4} M; i.e., at an [SH^-] at which the current is controlled by a combination of SH^- diffusive transport and the interfacial anodic reaction rate. A

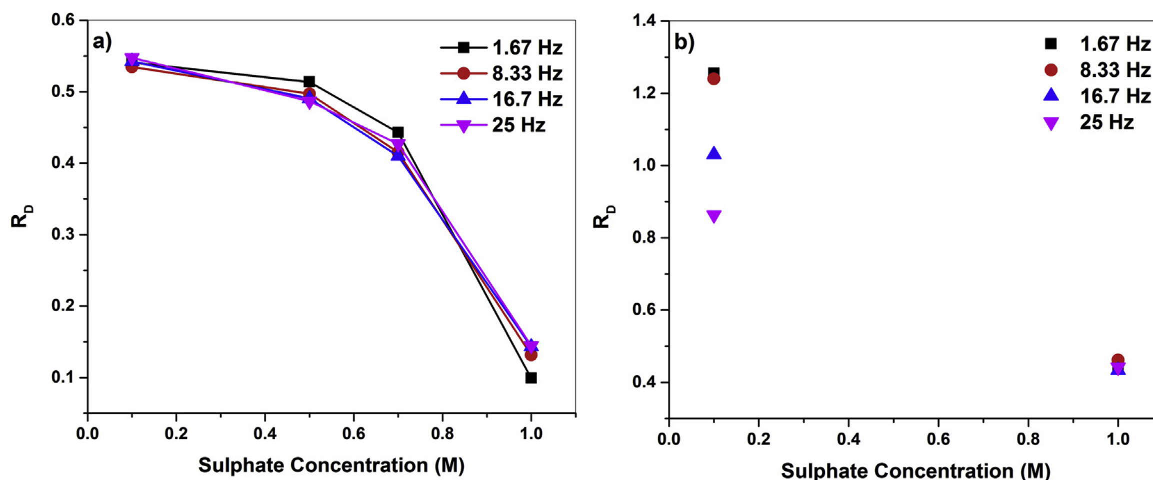

Fig. 9. Ratio (R_D) (defined in the text) as a function of [SO_4^{2-}] for various values of ω recorded in solutions of a) 10^{-4} M and b) 2.0×10^{-3} M SH^-.

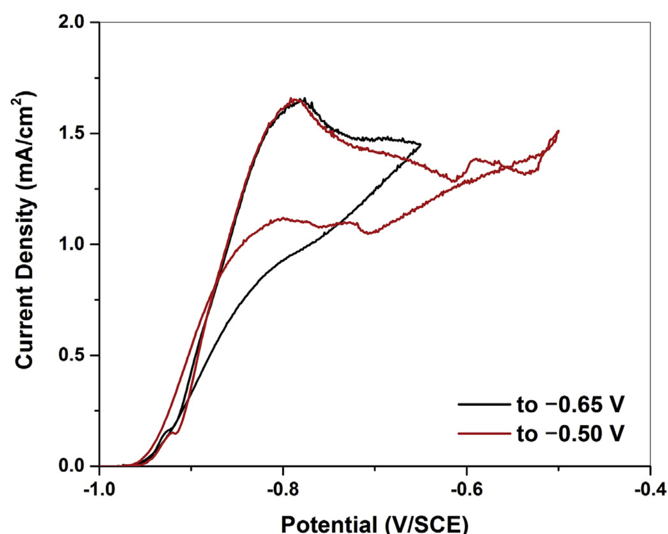

Fig. 10. Anodic region of CVs recorded in 2.0 M Cl^- + 0.5 M SO_4^{2-} + 2×10^{-3} M SH^- at ω = 25 Hz to different anodic limits.

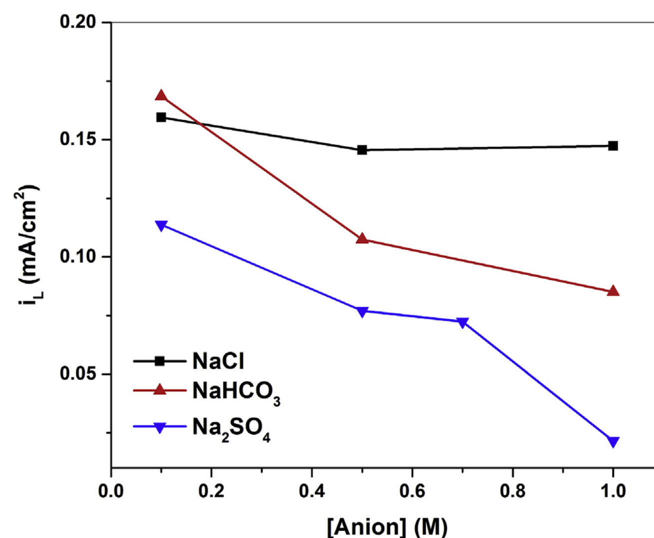

Fig. 11. Limiting currents at −0.73 V/SCE extracted from CVs recorded in a 10^{-4} M SH^- solution at ω = 25 Hz.

comparison at this [SH^-] avoided the complications encountered at higher [SH^-] when the properties of the Cu_2S deposit dominated the film growth behaviour. As noted above in the presence of Cl^- at this [SH^-], the film formation process was less dramatically influenced by [Cl^-] than at the lower [SH^-] of 5×10^{-5} M. Also, the influence of ionic strength on the film growth process appeared minor compared to that observed at the lower and higher [SH^-]. This is apparent in Fig. 11, where the current changed only slightly as the [Cl^-] increased. While SO_4^{2-} will have a considerably larger effect on the ionic strength than the singularly charged HCO_3^- and Cl^-, the behaviour observed indicated the dominant effect of SO_4^{2-} was in suppressing the Cu_2S film growth rate, most likely via competition for adsorption sites.

4. Summary and conclusions

- The effect of the anions (Cl^-, SO_4^{2-}, HCO_3^-) on the anodic formation of Cu_2S films on Cu has been studied voltammetrically.
- At low ionic strengths and [SH^-] ≤ 10^{-4} M, anodic film growth was, at least partially, controlled by ion transport in the porous network of the film. When the ionic strength was increased, the electric field within the pores was decreased leading to a decrease in pore resistance and a larger potential gradient across the Cu/solution interface at the base of pores, with the result that control of film growth switched to the anodic reaction on the Cu surface.
- At higher [SH^-] (>10^{-3} M) the film growth process became controlled by the properties of the film with ionic migration remaining rate controlling even at high ionic strength. This was attributed to the compact nature of the film with tighter porosity at these high [SH^-]. At sufficiently high applied potentials the film became protective but not completely passive.
- Besides changing the film growth kinetics by influencing the ionic strength and, hence, the distribution of the applied potential across the Cu/film layer, anions (Cl^-, SO_4^{2-}, HCO_3^-) compete with SH^- for adsorption sites on the Cu surface, thereby interfering with the initial electron transfer step (to produce $Cu(SH)_{ads}$) necessary for Cu_2S film formation.
- The ability of anions to suppress porous film growth increased in the order Cl^- < HCO_3^- < SO_4^{2-} under electrochemically-controlled conditions. This may be attributable to strong co-adsorption of SO_4^{2-} and H_2O on the Cu surface. Alternatively,

the weaker influence of Cl^- may be attributable to a synergistic influence of Cl^- and SO_4^{2-} in producing transportable Cu^I species.
- These results demonstrate that the anodic formation of Cu_2S on Cu did not proceed via a nucleation and growth process as claimed by others [31].

Acknowledgement

This project was funded by the Swedish Nuclear Fuel and Waste Management Company (SKB, Solna, Sweden), Posiva Oy (Olkiluoto, Finland) and the Nuclear Waste Management Organization (Toronto, Canada). The authors are grateful to Christina Lilja (SKB) and Fraser King (Integrity Corrosion Consulting, Nanaimo, BC, Canada) for many helpful discussions and suggestions.

References

[1] D.W. Shoesmith, Assessing the corrosion performance of high-level nuclear waste containers, Corrosion 62 (8) (2006) 703–722.
[2] F. King, C. Lilja, K. Pedersen, P. Pitkänen, M. Vähänen, An Update of the State-Of-The-Art Report on the Corrosion of Copper under Expected Conditions in a Deep Geologic Repository, Technical report for Swedish Nuclear Fuel and Waste Management Company, 2010. TR-10-67.
[3] F. King, C. Lilja, M. Vähänen, Progress in the understanding of the long-term corrosion behaviour of copper canisters, J. Nucl. Mater. 438 (1–3) (2013) 228–237.
[4] F. King, Corrosion of Copper in Alkaline Chloride Environments, Technical report for Swedish Nuclear Fuel and Waste Management Company, 2002. TR-02-25.
[5] R. Sandström, H.C.M. Andersson, The effect of phosphorus on creep in copper, J. Nucl. Mater. 372 (1) (2008) 66–75.
[6] J. Chen, Z. Qin, D.W. Shoesmith, Kinetics of corrosion film growth on copper in neutral chloride solutions containing small concentrations of sulfide, J. Electrochem. Soc. 157 (10) (2010) C338–C345.
[7] E.-L. Tullborg, J. Smellie, A.-C. Nilsson, M.J. Gimeno, L.F. Auqué, V. Brüchert, J. Molinero, SR-site – Sulphide Content in the Groundwater at Forsmark, Technical report for Swedish Nuclear Fuel and Waste Management Company, 2010. TR-10-39.
[8] J. Chen, Z. Qin, T. Martino, D.W. Shoesmith, Effect of chloride on Cu corrosion in anaerobic sulphide solutions, Corros. Eng. Sci. Technol. 52 (2017) 40–44.
[9] J. Chen, Z. Qin, T. Martino, D.W. Shoesmith, Non-uniform film growth and micro/macro-galvanic corrosion of copper in aqueous sulphide solutions containing chloride, Corros. Sci. 114 (2017) 72–78.
[10] J. Chen, Z. Qin, T. Martino, M. Guo, D.W. Shoesmith, Copper transport and sulphide sequestration during copper corrosion in anaerobic aqueous sulphide solutions, Corros. Sci. 131 (2018) 245–251.
[11] M. Guo, J. Chen, T. Martino, M. Biesinger, J.J. Noël, D.W. Shoesmith, The susceptibility of copper to pitting corrosion in borate-buffered aqueous solutions containing chloride and sulphide, J. Electrochem. Society 166 (15) (2019) C550–C558.
[12] J. Chen, Z. Qin, D.W. Shoesmith, Key parameters determining structure and properties of sulphide films formed on copper corroding in anoxic sulphide solutions, Corros. Eng. Sci. Technol. 49 (6) (2014) 415–419.
[13] T. Martino, R. Partovi-Nia, J. Chen, Z. Qin, D.W. Shoesmith, Mechanisms of film growth on copper in aqueous solutions containing sulphide and chloride under voltammetric conditions, Electrochim. Acta 127 (2014) 439–447.
[14] T. Martino, J. Chen, Z. Qin, D.W. Shoesmith, The kinetics of film growth and their influence on the susceptibility to pitting of copper in aqueous sulphide solutions, Corros. Eng. Sci. Technol. 52 (2017) 61–64.
[15] C.F. Dong, F.X. Mao, S.J. Gao, S. Sharifi-Asl, P. Lu, D.D. Macdonald, Passivity breakdown on copper: influence of temperature, J. Electrochem. Soc. 163 (13) (2016) C707–C717.
[16] F.X. Mao, C.F. Dong, S. Sharifi-Asl, P. Lu, D.D. Macdonald, Passivity breakdown on copper: influence of chloride ion, Electrochim. Acta 144 (2014) 391–399.
[17] D.C. Kong, C.F. Dong, X.Q. Ni, A.N. Xu, C. He, K. Xiao, X.G. Li, Long-term polarisation and immersion for copper corrosion in high-level nuclear waste environment, Mater. Corros. 68 (10) (2017) 1070–1079.
[18] D.C. Kong, C.F. Dong, K. Xiao, X.G. Li, Effect of temperature on copper corrosion in high-level nuclear waste environment, T. Nonferr. Metal. Soc. 27 (6) (2017) 1431–1438.
[19] D.C. Kong, C.F. Dong, A.N. Xu, C. He, X.G. Li, The stability of passive film growth on copper in anaerobic sulphide solutions, Corros. Eng. Sci. Technol. 52 (3) (2017) 188–194.
[20] T. Martino, J. Smith, J. Chen, Z. Qin, J.J. Noël, D.W. Shoesmith, The properties of electrochemically-grown copper sulfide films, J. Electrochem. Soc. 166 (2) (2019) C9–C18.
[21] P. Broekmann, M. Wilms, M. Kruft, C. Stuhlmann, K. Wandelt, In-situ STM investigation of specific anion adsorption on Cu(111), J. Electroanal. Chem. 467 (1) (1999) 307–324.
[22] D.W. Smith, Ionic hydration enthalpies, J. Chem. Educ. 54 (9) (1977) 540–542.
[23] M. Lennartz, P. Broekmann, M. Arenz, C. Stuhlmann, K. Wandelt, Sulfate adsorption on Cu(111) studied by in-situ IRRAS and STM: revealing the adsorption site and desorption behavior, Surf. Sci. 442 (2) (1999) 215–222.
[24] W.-H. Li, R.J. Nichols, An in situ STM study of sulphate adsorption on copper(111) in acidic aqueous electrolytes, J. Electroanal. Chem. 456 (1) (1998) 153–160.
[25] G. Niaura, A. Malinauskas, Surface-enhanced Raman spectroscopy of ClO_4^- and SO_4^{2-} anions adsorbed at a Cu electrode, J. Chem. Soc., Faraday Trans. 94 (15) (1998) 2205–2211.
[26] V.I. Birss, G.A. Wright, The kinetics of the anodic formation and reduction of phase silver sulfide films on silver in aqueous sulfide solutions, Electrochim. Acta 26 (12) (1981) 1809–1817.
[27] V.I. Birss, G.A. Wright, The kinetics of silver iodide film formation on the silver anode, Electrochim. Acta 27 (10) (1982) 1439–1443.
[28] V.I. Birss, G.A. Wright, The kinetics of silver bromide film formation on the silver anode, Electrochim. Acta 27 (10) (1982) 1429–1437.
[29] X. Zhang, S. Stewart, D.W. Shoesmith, J.C. Wren, Interaction of aqueous iodine species with Ag_2O/Ag surfaces, J. Electrochem. Soc. 154 (4) (2007) F70–F76.
[30] A. Spänig, P. Broekmann, K. Wandelt, Atomic structure of adsorbed sulfide on Cu(111) in acidic solution: in situ STM studies, Electrochim. Acta 50 (21) (2005) 4289–4296.
[31] B. Scharifker, R. Rugeles, J. Mozota, Electrocrystallization of copper sulphide (Cu_2S) on copper, Electrochim. Acta 29 (2) (1984) 261–266.